Published in final edited form as:
J Neurochem. 2009 April ; 109(2): 494–501. doi:10.1111/j.1471-4159.2009.05967.x.

In Situ 3D MR Metabolic Imaging of Microwave-Irradiated Rodent Brain: A New Tool for Metabolomics Research

Robin A. de Graaf, **Golam M.I. Chowdhury**, **Peter B. Brown**, **Douglas L. Rothman**, and **Levin L. Behar**
Magnetic Resonance Research Center Yale University, School of Medicine New Haven, Connecticut, USA

Abstract

The rapid elevation in rat brain temperature achieveable with focused beam microwave irradiation (FBMI) leads to a permanent inactivation of enzymes, thereby minimizing enzyme-dependent post mortem metabolic changes. An additional characteristic of FBMI is that the NMR properties of the tissue are close to those of the *in vivo* condition and remain so for at least 12 hours. These features create an opportunity to develop MRI and MRS on microwave-irradiated samples into a technique with a resolution, coverage and sensitivity superior to any experiment performed directly *in vivo*. Furthermore, when combined with pre-FBMI infusion of ^{13}C-labeled substrates, like [1-^{13}C]-glucose, the technique can generate maps of metabolic fluxes, like the TCA and glutamate-glutamine neurotransmitter cycle fluxes at an unprecedented spatial resolution.

Keywords

Microwave fixation; *in situ* NMR spectroscopy; rat brain

INTRODUCTION

The spatial resolution of *in vivo* ^{1}H NMR spectroscopy has dramatically increased with higher magnetic fields, improved RF coils and optimized acquisition strategies. However, even on state-of-the-art MR systems, the spatial resolution of *in vivo* NMR spectroscopy studies on animal brain is still relatively coarse (> 10 μL) compared to typical anatomical structures, leading to significant partial volume effects. For low-concentration metabolites like γ-amino butyric acid (GABA), the spatial resolution is reduced even further in order to compensate for the reduced amount of signal. The sensitivity and hence spatial resolution at high magnetic fields can essentially only be increased by (1) increased measurement time (averages) or (2) improved RF coil design. Surface coil reception can locally improve sensitivity at the cost of reduced sample coverage. While this effect can partially be mitigated by phased-array coils, the obtainable *in vivo* sensitivity is ultimately limited by the physiological (i.e. temporal) stability of the animal.

Correspondence to: Robin A. de Graaf, Ph. D., MRRC, Yale University, Departments of Diagnostic Radiology and Biomedical Engineering, TAC, N145, 300 Cedar Street, P. O. Box 208043, New Haven, CT 06520-8043, Tel : (203)-785-6203, Fax : (203)-785-6643, robin.degraaf@yale.edu.

AUTHOR CONTRIBUTIONS

R. A. G. designed the study, performed all *in vivo* and *in situ* MR studies, processed all data and wrote the manuscript. G. M. I. C. performed the microwave fixation. P. B. B. designed and created the ^{1}H/^{13}C volume RF coil. D. L. R. and K. L. B. conceived the method and provided valuable inputs throughout the study.

Many neurochemicals, like cyclic nucleotides, ATP, glucose, lactate and certain neurotransmitters, like GABA, undergo rapid post mortem alterations due to on-going metabolism, thereby giving a distorted characterization of *in vivo* metabolism. These alterations can be minimized by methods that reduce or even completely halt post mortem metabolism rapidly. In rodent studies the most commonly used methods of enzyme inactivation involves rapid *in situ* freezing with liquid nitrogen, such as freeze-blowing (Veech et al. 1973), freeze-clamping (Bolwig and Quistorff 1973), or funnel-freezing (Ponten et al. 1973). However, these methods suffer from limited control of region specificity, reactivation of enzymes upon thawing and poorer preservation of deeper brain regions due to the finite speed of the freezing front before blood flow ceases. Obtaining tissue from well-defined brain regions from the frozen cranium is both laborious and challenging, requiring the use of a cryostat for dissection of non-superficial cortical regions.

Since the early 1970s focused beam microwave irradiation (FBMI) has been used as an alternative for the preparation of post mortem tissue samples on small laboratory animals (Stavinoha et al. 1970). Using a dedicated FBMI device with 5 – 10 kW output power, the technique rapidly (0.5 – 1.5 s) elevates brain temperature to 80 – 90 °C. This leads to a permanent inactivation of enzymes, thereby minimizing enzyme-dependent post mortem metabolic changes.

Comparisons following FBMI and freezing methods have been reported for several compounds in brain tissues that are characterized by rapid post-mortem concentration changes, including acetylcholine (Stavinoha et al. 1973), ATP (Delaney and Geiger 1996), cyclic AMP (Schmidt et al. 1971; Balcom et al. 1975), GABA (Balcom et al. 1975; Elekes et al. 1986; Miller et al. 1990), glutathione (Miller et al. 1990), glycogen (Kong et al. 2002; Morgenthaler et al. 2006) and neuropeptides (Parkin et al. 2005). In all cases the metabolite levels found with FBMI were much closer to the known or suspected *in vivo* levels than with the freezing methods, supporting the contention that FBMI minimizes post mortem neurochemical alterations. It should be noted that many of the mentioned metabolites, like cyclic AMP, are not NMR observable due to their low concentration or their relaxation properties.

Here we explore the use of *in situ* NMR on microwave-irradiated samples to improve the sensitivity/resolution by both mechanisms, while maintaining the metabolic profile and structural tissue integrity of the *in vivo* situation. Besides the minimal alteration of post mortem metabolite levels, two additional benefits of FBMI are that the inactivation of enzymes is permanent (i.e. enzymes can not be re-activated) and that the NMR properties of the tissue are close to those of the *in vivo* condition (i.e. the tissue is not frozen). These two additional features create an opportunity to develop NMR spectroscopy on microwave-irradiated samples into a technique that can generate spatial maps of *in vivo* metabolism with a resolution, coverage and sensitivity superior to any NMR experiment performed directly *in vivo*. Presented results will demonstrate that the microwave-irradiated samples are metabolically and structurally stabile for at least 12 hours, providing a large time-window in which to acquire high-resolution maps of *in vivo* metabolism.

MATERIALS AND METHODS

All *in vivo* and *in situ* experiments were performed on a 11.74 T Magnex magnet (Magnex Scientific Ltd, Oxford, UK) interfaced to a Bruker Avance Spectrometer (Bruker Instruments, Billerica, MA) equipped with 9.0 cm diameter Magnex gradients capable of switching 395 mT/m in 180 μs. For *in vivo* experiments RF transmission and reception was performed with a 14 mm diameter surface coil tuned to the proton NMR frequency (499.8 MHz). For all *in situ* experiments RF transmission and reception was achieved with a four-turn, 25 mm diameter solenoidal coil of 45 mm length. Heteronuclear spectral editing and broadband decoupling was

performed with a 28 mm diameter Helmholtz coil (29 mm coil separation) tuned to the carbon-13 NMR frequency (125.7 MHz) and placed outside of the proton NMR coil.

For the *in situ* studies ten male Sprague-Dawley rats (206 ± 11 g, mean SD) were euthanized by microwave irradiation using the commercially available 10 kW Muromachi Microwave Fixation System (Stoelting Co, Wood Dale, IL) in accordance to the guidelines established by the Yale Animal Care and Use Committee. Under light halothane anesthesia the animals were place in dedicated animal holders to ensure proper positioning within the device. The head of the animal was constrained by a narrow, water-cooled area with dimensions similar to a rat head of size 180 – 220 g. In order to prevent the animal from pulling out of the device, the body was blocked at the tail end. The optimal fixation power and duration represents a compromise between stopping metabolism and the generation of microscopic air bubbles that severely compromise the B_0 magnetic field homogeneity (see Results). The current group of animals were irradiated at 4.5 kW in 1.2 s, which essentially halted cerebral metabolism for at least 12 hours (see Results), while generating only a small number of air bubbles. Following microwave fixation all extracranial tissues were removed after which the skull and brain were immersed in deuterium oxide (17 mm diameter, 55 mm long tube) to minimize magnetic susceptibility artifacts created at air-brain interfaces. Since brain water exchanges with deuterium oxide over the span of hours, in later studies the deuterium oxide was replaced with Fluorinert FC-43 (3M, St. Paul, MN), an inert, clear fluid with a magnetic susceptibility close to water (Olson et al. 1995). The sample tube fitted snugly into the proton solenoidal coil for optimal NMR sensitivity.

For *in vivo* studies three male Sprague-Dawley rats (210 ± 13 g, mean ± SD) were prepared in accordance to the guidelines established by the Yale Animal Care and Use Committee. The animals were tracheotomized and ventilated with a mixture of 70 % nitrous oxide and 28.5 % oxygen under 1.5 % halothane anesthesia. A femoral artery was cannulated for monitoring of blood gases (pO_2, pCO_2), pH and blood pressure. Physiological variables were maintained within normal limits by small adjustments in ventilation (pCO_2 = 33–45 mm Hg; pO_2 > 120 mm Hg; pH = 7.20–7.38; blood pressure = 90–110 mm Hg). After all surgery was completed, anesthesia was maintained by 0.3 – 0.7 % halothane in combination with 70 % nitrous oxide. During NMR experiments animals were restrained in a head holder, while additional immobilization was obtained with d-tubocurarine chloride (0.5 mg/kg/40 mins, i.p.). The core temperature was measured with a rectal thermosensor and was maintained at 37 ± 1 °C by means of a heated water pad.

The magnetic field homogeneity was optimized through MRI-based B_0 mapping (Koch et al. 2006). Briefly, four gradient-echo images (TR = 1000 ms, 128 × 64 over 38.4 × 19.2 mm, 30 slices over 18.0 mm) with different echo-time TE + τ (with τ = 0, 0.33, 1.0 and 3.0 ms) were acquired. The phase of each image was determined relative to the first image. Temporal phase-unwrapping, under the assumption that the phase in the second image is within the range [$-\pi$, $+\pi$], yielded a linear (phase, time τ) curve. The slope, obtained by linear regression, is then proportional to the magnetic field offset ΔB_0. The measured ΔB_0 map was fitted with first and second spherical harmonics across the entire brain after which the shims could be updated.

Single volume ^{1}H NMR spectroscopy was performed with LASER (Slotboom et al. 1991; Garwood and DelaBarre 2001) with TR/TE = 4000/14 ms on a 16 μL volume positioned in the cerebral cortex. Water suppression was achieved with SWAMP (de Graaf and Nicolay 1998), an adiabatic analog of CHESS (Haase et al. 1985).

Multi-slice ^{1}H MRSI (TR/TE = 3500/10 ms) was performed with a double spin-echo sequence consisting of a 1 ms Shinnar-Le Roux optimized excitation pulse (Pauly et al. 1991) and a pair of 1 ms adiabatic full passage refocusing pulses. 11 slices (1 mm thickness) were selected and

encoded over a circular k-space sampling grid (284 total phase-encoding steps, FOV = 20 × 20 mm), giving a nominal MRSI voxel size of 1 μL. Since all extracranial tissues were removed, no outer volume suppression was required.

RESULTS

One of the requirements for meaningful *in situ* NMR of microwave fixed brains is structural integrity of the tissue. T_2-weighted MRI is sensitive to the formation of edema, whereas diffusion tensor imaging (DTI) can be used to assess integrity of white matter fiber tracts. Figure 1 shows high-resolution (75 μm and 60 μm in-plane resolution for A and B/C, respectively) T_2-weighted images (TE = 35 ms) of microwave-irradiated rat brain. Excellent soft-tissue contrast was apparent without any noticeable signs of edema formation or tissue degradation. This is essential for a variety of high-resolution MRI applications to characterize disease progression, like plaque formation in Alzheimer's disease (Jack et al. 2005). Figure 2 shows a typical DTI data set, which reveals strong white matter anisotropy (fractional anisotropy = 0.7 – 0.8), mild and uniform anisotropy in gray matter (FA = 0.15 – 0.25), and essentially isotropic diffusion in CSF (FA ~ 0). These diffusion characteristics are identical to those found in rat brain *in vivo*, thereby further supporting the notion that FBMI does not significantly affect tissue structure.

A prime concern in the development of *in situ* NMR on microwave irradiated samples is the temporal stability of the samples. Fig. 3A shows a localized ^{1}H-NMR spectrum from rat brain, 60 min following microwave irradiation. The spectrum closely resembles an *in vivo* ^{1}H brain spectrum (Fig. 3B). Low levels of lactate and GABA, high levels of phosphocreatine and common ratios of *N*-acetyl aspartate (NAA), total creatine and total choline are all indicative of minimal post mortem changes in metabolite levels. A ^{1}H NMR spectrum of halothane-euthanized rat brain is shown in Fig. 3D for comparison. The ^{1}H NMR spectra from microwave-irradiated rat brain show remarkably little change in the first 12–16 hours (Fig. 3C). After 16 hours, the total choline, taurine, lactate, and alanine resonances increase, indicating that not all enzymatic activity has been completely halted. However, a time window of 16 hours typically represents a maximum measurement time due to limited MR system availability and diminishing S/N returns. Figure 4 presents the absolute metabolite concentrations of the different spectra using LCmodel spectral fitting and assuming a 10 mM concentration for total creatine.

Figure 5 shows one of the metabolic applications whereby the combination of intravenous infusion of ^{13}C-labeled substrates and microwave irradiation can be used to obtain dynamic metabolic information. Figure 5B shows ^{1}H (top) and edited ^{1}H-[^{13}C]-NMR spectra from a 1.0 μL volume extracted from a multi-slice 20 × 20 MRSI data set acquired in circa 6 hours following 2 hours of intravenous infusion of [1,6-$^{13}C_2$]-glucose and subsequent microwave irradiation. The position of the volume is indicated in the MR image shown in Fig. 5A. Despite the small voxel size of 1.0 μL, the sensitivity is adequate to detect the formation of [4-^{13}C]-glutamate, [4-^{13}C]-glutamine and other ^{13}C-labeled products. The high spatial resolution also allows the generation of metabolic maps as shown in Figs. 5E and F for [4-^{13}C]-glutamate and [4-^{13}C]-glutamine. Alternatively spectra from multiple voxels can be co-added to obtain high S/N data as shown in Fig. 5D for ^{1}H and edited ^{1}H-[^{13}C]-NMR spectra of the hippocampus as indicated in Fig. 5C. By repeating the studies shown in Fig. 5 for different infusion times (on different animals), the full dynamic turnover time course can be obtained at a spatial resolution and sensitivity that is several times higher than direct *in vivo* detection. Combined with mathematical modeling procedures, absolute fluxes can be assessed for a number of important metabolic pathways (e.g. tricarboxylic acid cycle) in neurons and astroglia (de Graaf et al. 2003).

Microwave irradiation generated entrapped air bubbles on a limited number of animals, of which Fig. 6 shows a typical example. When present, the air bubbles typically formed at the boundary of ventricles and brain parenchyma. While air bubbles generally do not prevent high-resolution anatomical MRI (Fig. 6A), they do perturb the magnetic field over a significant area (Fig. 6B). Since ^{1}H and edited ^{1}H-[^{13}C]-NMR spectroscopy rely on a highly homogeneous magnetic field, the presence of air bubbles prevents the acquisition of high quality data in the immediate area surrounding the air bubbles. Generally it was observed that the majority of air bubbles disappear in a matter of hours following microwave irradiation, presumably due to water accumulation or reabsorption.

DISCUSSION

Here we have demonstrated that microwave-irradiated rat brain possesses the structural integrity and temporal stability to allow the acquisition of high-resolution *in situ* MR spectra and images that reflect the *in vivo* condition. However, with improved RF coil design and greatly increased acquisition times, the *in situ* results can be obtained at a sensitivity which greatly exceeds that of direct *in vivo* acquisition.

The ^{1}H NMR spectroscopy results of Fig. 3 and Fig. 4 indicate that FBMI does rapidly inactivate cerebral enzymes. Common post mortem changes observed by ^{1}H NMR (Fig 3D) are a very fast creatine-kinase-catalyzed conversion of phosphocreatine to creatine, a fast accumulation of lactic acid by anaerobic glycolysis and a glutamate-decarboxylase-catalyzed formation of GABA. In the *in situ* ^{1}H NMR spectra from microwave-irradiated rat brain none of these three processes were observed. However, at the later time points (≥16 hours) some spectral changes were seen, in particular a small elevation in lactate, alanine, and taurine/total choline, and a reduction in NAA. Since the samples were measured at room temperature under non-sterile conditions, the metabolic changes could possibly be attributed to bacterial growth and tissue breakdown. However, the significant increase in taurine after 16 hours is puzzling because previous postmortem measurements of amino acids in rat and human brain tissue maintained at room temperature for up to 4 hours or human brain autopsy specimens stored at 0–4°C for up to 120 hours showed taurine levels to be relatively stable (Perry et al. 1981). Whether potential renaturation of some heat inactivated enzymes could occur is not known, but studies confined to the first 12 hours after microwave irradiation can be expected to be highly stable.

While direct ^{1}H NMR spectroscopy demonstrates metabolic stability, the local cellular environment could have significantly changed by the intense heat generated by the microwave irradiation. While DTI provides the first indication that this is not the case, cellular integrity can be investigated further with diffusion-weighted ^{1}H NMR spectroscopy (Nicolay et al. 2001). Diffusion-weighted ^{1}H MRS of intracellular metabolites is sensitive to restrictive barriers, such as cell membranes and sub-cellular organelles and can therefore provide information about cellular and sub-cellular integrity non-invasively. This will be the subject of future studies

The results presented in Fig. 5 demonstrate that high-spatial-resolution information on dynamic metabolic turnover can be obtained when FBMI is combined with *in vivo* ^{13}C-labeled substrate infusion. Absolute metabolic fluxes, like the TCA cycle flux, can be obtained by either measuring metabolic turnover at an early time point or by measuring multiple time points on multiple animals. In the first case, metabolic fluxes can simply be obtained from linear, initial slope estimates. In the second case it becomes important to either properly co-register between different animals or to perform the analysis on well-defined regions-of-interest.

The main obstacle remaining for consistent whole brain coverage is the formation of small air pockets during microwave irradiation, presumably due to rapid vaporization of tissue water in local hotspots. While these air pockets do not impede conventional processing of microwave-irradiated tissue samples, i.e. tissue dissection, metabolite extraction and subsequent analysis by high-resolution NMR (e.g. (Chowdhury et al. 2008)) or other analytical methods, it can strongly degrade the quality of ^{1}H MRSI data due to the strong disturbance of the local magnetic field homogeneity (see Fig. 6B). The formation of small air pockets is difficult to eliminate completely, as the number and position can vary somewhat despite constant animal body weight and FBMI settings. There is, however, a fairly consistent relationship between the total microwave irradiation power and the number of air pockets. The final setting of the irradiation power (1.2 s, 4.5 kW) was therefore chosen as to minimize the number of air pockets while still halting cerebral metabolism.

In conclusion, FBMI in combination with *in situ* MRI and MRS is a novel method to obtain high-resolution, high-sensitivity structural and metabolic information from rodent brain with 3-dimensional full brain coverage. Intravenous infusion of ^{13}C-labeled glucose or acetate prior to FBMI, substrates which target neuronal or glial metabolism respectively, can be used to provide cell-specific dynamic rate information on mitochondrial energetics and neuron-glia substrate trafficking at here-to-fore unprecedented spatial resolution. The ability to anatomically register the metabolic images with *in situ* immunohistochemistry of expressed proteins, phosphoproteins, and neuropeptides, which are preserved by FBMI (Theodorsson et al. 1990; O'Callaghan and Sriram 2004; Che et al. 2005; Hunsucker et al. 2008) and readily measured after the metabolic image is obtained, will add new dimensions to the versatility and information rich potential of this new metabolomics approach.

Abbreviations used

CHESS	chemical shift selective
FA	fractional anisotropy
FBMI	focused beam microwave irradiation
FOV	field-of-view
LASER	localization by adiabatic spin-echo refocusing
MRSI	magnetic resonance spectroscopic imaging
RF	radiofrequency
SWAMP	selective water suppression with adiabatic modulated pulses
TE	echo-time
TCA	tricarboxylic acid
TR	repetition time

Acknowledgments

This research was supported by NIH grant R21-CA118503 and R01-DK027121. The authors thank Bei Wang for expert animal preparation.

REFERENCES

Balcom GJ, Lenox RH, Meyerhoff JL. Regional gamma-aminobutyric acid levels in rat brain determined after microwave fixation. J Neurochem 1975;24:609–613. [PubMed: 1123612]

Bolwig TG, Quistorff B. *In vivo* concentration of lactate in the brain of conscious rats before and during seizures: a new ultra-rapid technique for the freeze-sampling of brain tissue. J Neurochem 1973;21:1345–1348. [PubMed: 4761715]

Che FY, Lim J, Pan H, Biswas R, Fricker LD. Quantitative neuropeptidomics of microwave-irradiated mouse brain and pituitary. Mol Cell Proteomics 2005;4:1391–1405. [PubMed: 15970582]

Chowdhury GMI, Banasr M, de Graaf RA, Rothman DL, Behar KL, Sanacora G. Chronic riluzole treatment increases glucose metabolism in rat prefrontal cortex and hippocampus. J Cereb Blood Flow Metab. 2008 in press.

de Graaf RA, Nicolay K. Adiabatic water suppression using frequency selective excitation. Magn Reson Med 1998;40:690–696. [PubMed: 9797151]

de Graaf RA, Mason GF, Patel AB, Behar KL, Rothman DL. *In vivo* ^{1}H-[^{13}C]-NMR spectroscopy of cerebral metabolism. NMR Biomed 2003;16:339–357. [PubMed: 14679499]

Delaney SM, Geiger JD. Brain regional levels of adenosine and adenosine nucleotides in rats killed by high-energy focused microwave irradiation. J Neurosci Methods 1996;64:151–156. [PubMed: 8699875]

Elekes I, Patthy A, Lang T, Palkovits M. Concentrations of GABA and glycine in discrete brain nuclei. Stress-induced changes in the levels of inhibitory amino acids. Neuropharmacology 1986;25:703–709. [PubMed: 3092127]

Garwood M, DelaBarre L. The return of the frequency sweep: designing adiabatic pulses for contemporary NMR. J Magn Reson 2001;153:155–177. [PubMed: 11740891]

Haase A, Frahm J, Hanicke W, Matthaei D. ^{1}H NMR chemical shift selective (CHESS) imaging. Phys Med Biol 1985;30:341–344. [PubMed: 4001160]

Hunsucker SW, Solomon B, Gawryluk J, Geiger JD, Vacano GN, Duncan MW, Patterson D. Assessment of post-mortem-induced changes to the mouse brain proteome. J Neurochem 2008;105:725–737. [PubMed: 18088372]

Jack CR Jr. Wengenack TM, Reyes DA, Garwood M, Curran GL, Borowski BJ, Lin J, Preboske GM, Holasek SS, Adriany G, Poduslo JF. In vivo magnetic resonance microimaging of individual amyloid plaques in Alzheimer's transgenic mice. J Neurosci 2005;25:10041–10048. [PubMed: 16251453]

Koch KM, McIntyre S, Nixon TW, Rothman DL, de Graaf RA. Dynamic shim updating on the human brain. J Magn Reson 2006;180:286–296. [PubMed: 16574443]

Kong J, Shepel PN, Holden CP, Mackiewicz M, Pack AI, Geiger JD. Brain glycogen decreases with increased periods of wakefulness: implications for homeostatic drive to sleep. J Neurosci 2002;22:5581–5587. [PubMed: 12097509]

Miller JM, Jope RS, Ferraro TN, Hare TA. Brain amino acid concentrations in rats killed by decapitation and microwave irradiation. J Neurosci Methods 1990;31:187–192. [PubMed: 2329838]

Morgenthaler FD, Koski DM, Kraftsik R, Henry PG, Gruetter R. Biochemical quantification of total brain glycogen concentration in rats under different glycemic states. Neurochem Int 2006;48:616–622. [PubMed: 16522343]

Nicolay K, Braun KP, de Graaf RA, Dijkhuizen RM, Kruiskamp MJ. Diffusion NMR spectroscopy. NMR Biomed 2001;14:94–111. [PubMed: 11320536]

O'Callaghan JP, Sriram K. Focused microwave irradiation of the brain preserves *in vivo* protein phosphorylation: Comparison with other methods of sacrifice and analysis of multiple phosphoproteins. J Neurosci Methods 2004;135:159–168. [PubMed: 15020100]

Olson DL, Peck TL, Webb AG, Magin RL, Sweedler JV. High-resolution microcoil 1H NMR for mass-limited nanoliter-volume samples. Science 1995;270:1967–1970.

Parkin MC, Wei H, O'Callaghan JP, Kennedy RT. Sample-dependent effects on the neuropeptidome detected in rat brain tissue preparations by capillary liquid chromatography with tandem mass spectrometry. Anal Chem 2005;77:6331–6338. [PubMed: 16194096]

Pauly J, Le Roux P, Nishimura D, Macovski A. Parameter relations for the Shinnar-Le Roux selective excitation pulse design algorithm. IEEE Trans Med Imaging 1991;10:53–65. [PubMed: 18222800]

Perry TL, Hansen S, Gandham SS. Postmortem changes of amino compounds in human and rat brain. J Neurochem 1981;36:406–410. [PubMed: 7463068]

Ponten U, Ratcheson RA, Salford LG, Siesjo BK. Optimal freezing conditions for cerebral metabolites in rats. J Neurochem 1973;21:1127–1138. [PubMed: 4761701]

Schmidt MJ, Schmidt DE, Robison GA. Cyclic adenosine monophosphate in brain areas: microwave irradiation as a means of tissue fixation. Science 1971;173:1142–1143. [PubMed: 4329179]

Slotboom J, Mehlkopf AF, Bovee WM. A single-shot localization pulse sequence suited for coils with inhomogneous RF fields using adiabatic slice-selective RF pulses. J Magn Reson 1991;95:396–404.

Stavinoha WB, Pepelko B, Smith PW. Microwave irradiation to inactivate cholinesterase in the rat brain prior to analysis for acetylcholine. Pharmacologist 1970;12:257.

Stavinoha WB, Weintraub ST, Modak AT. The use of microwave heating to inactivate cholinesterase in the rat brain prior to analysis for acetylcholine. J Neurochem 1973;20:361–371. [PubMed: 4698283]

Theodorsson E, Stenfors C, Mathe AA. Microwave irradiation increases recovery of neuropeptides from brain tissues. Peptides 1990;11:1191–1197. [PubMed: 1708137]

Veech RL, Harris RL, Veloso D, Veech EH. Freeze-blowing: a new technique for the study of brain *in vivo*. J Neurochem 1973;20:183–188. [PubMed: 4405707]

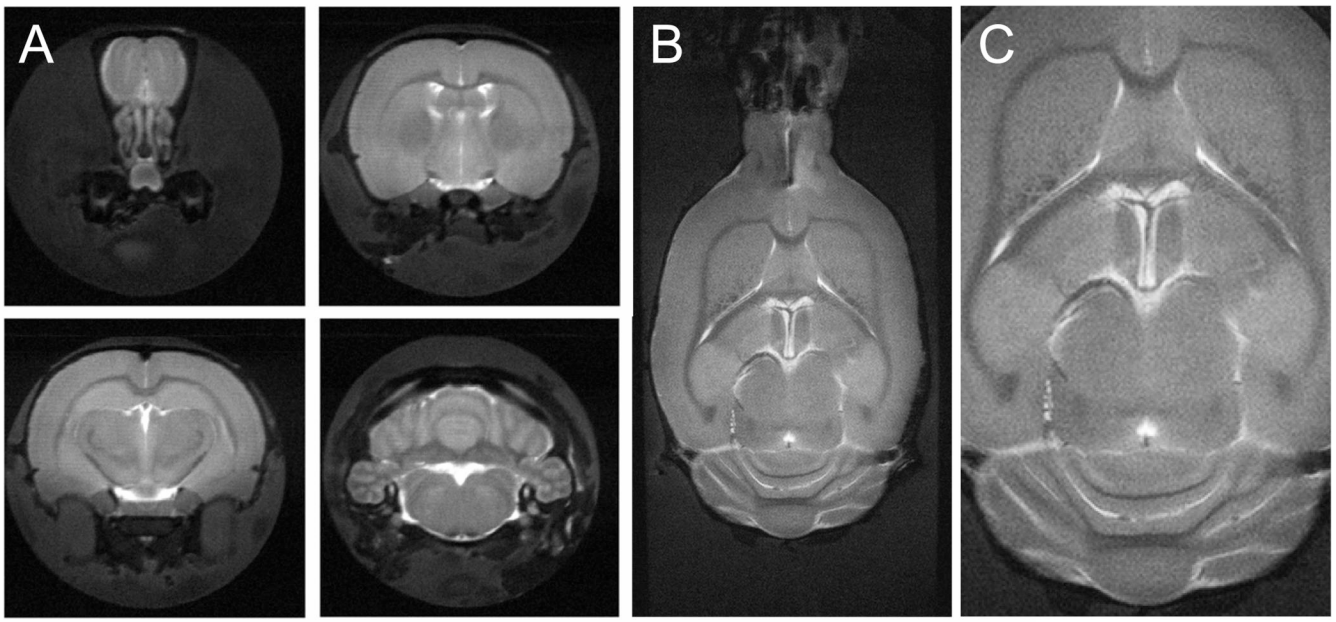

Figure 1.

Anatomical MR imaging on microwave-fixated rat brain. (A) Axial and (B/C) coronal T_2-weighted, multi-slice, multi-shot RARE images (TR/TE = 3500/35 ms, 32 segments) of microwave-irradiated rat brain acquired over 750 μm and 600 μm thick slices, respectively. 256 × 256 and 640 × 320 data matrices were acquired for A and B/C, over 19.2 × 19.2 and 38.4 × 19.2 mm FOVs, respectively. Excellent soft-tissue contrast partially demonstrates structural integrity of microwave-irradiated samples. Data were acquired in 40 min (A) and 90 min (B/C). (C) represents an expanded view of (B).

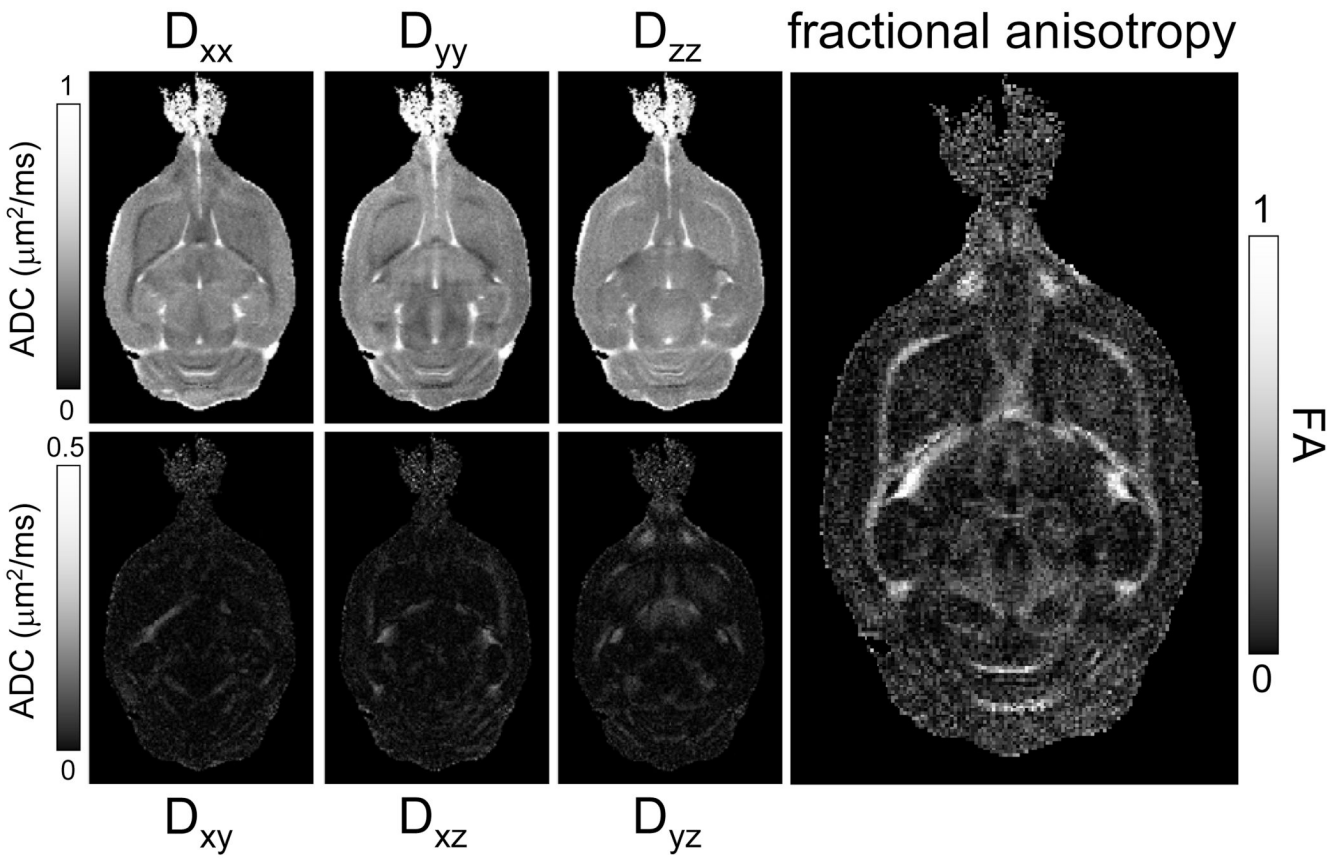

Figure 2.

Diffusion tensor imaging (DTI) on microwave-fixated rat brain. Data was acquired at a 120 × 120 μm in-plane resolution over 1000 μm thick slices. Diffusion maps were calculated using a SVD over 14 experiments (13 directions, b-value = 1.4 ms/μm^2 and 1 image with b = 0 ms/μm^2). White matter anisotropy is clearly visible in all six directional diffusion maps. This is further emphasized in the fractional anisotropy (FA) map, calculated from the three eigenvalues of the diffusion tensor. Excellent contrast between gray matter (FA ~ 0.2) and white matter (FA > 0.6) is visible.

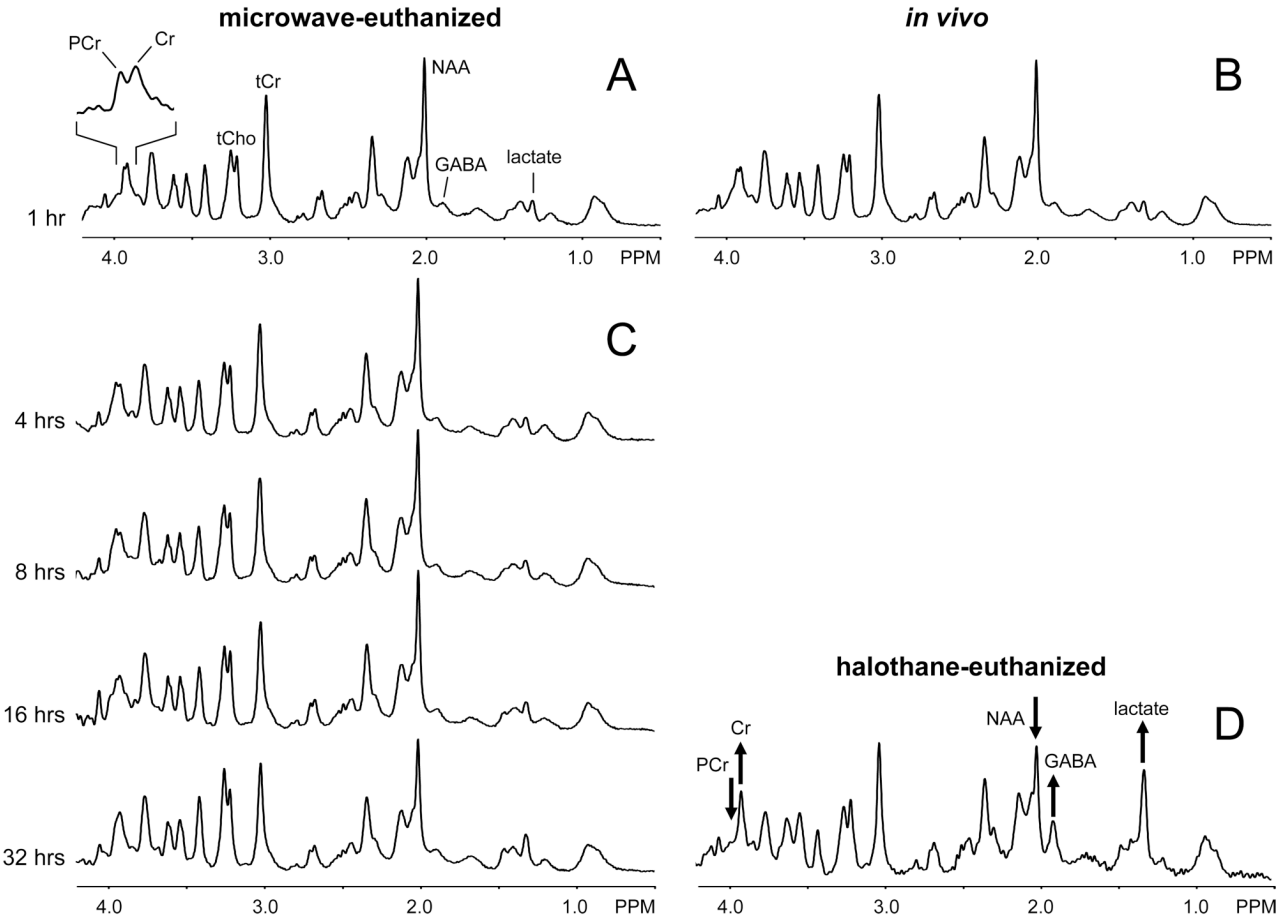

Figure 3.

Proton NMR spectroscopy on microwave-fixated rat brain *in situ* and rat brain *in vivo* and post mortem. (A) Localized ^{1}H NMR spectrum (16 μL, 10 min) of rat brain acquired 1 hour following 1.2 s, 4.5 kW microwave irradiation. (B) Localized ^{1}H NMR spectrum (24 μL, 5 min) of rat brain in vivo and (D) acquired 1 hour following euthanasia with 5% halothane. The microwave-irradiated ^{1}H NMR spectrum closely resembles the *in vivo* ^{1}H NMR spectrum. The hallmarks for post-mortem ^{1}H NMR changes present in (D), i.e. elevated lactate, GABA and creatine (Cr), reduced NAA and missing phosphocreatine (PCr), are noticeably absent from the spectrum in (A). This partially demonstrates the metabolic integrity of brain tissue following microwave irradiation. (C) Acquiring ^{1}H NMR spectra longitudinally over 32 hours shows remarkable stability for 12–16 hours. In the very late time points small changes in taurine/total choline, NAA and lactate become noticeable.

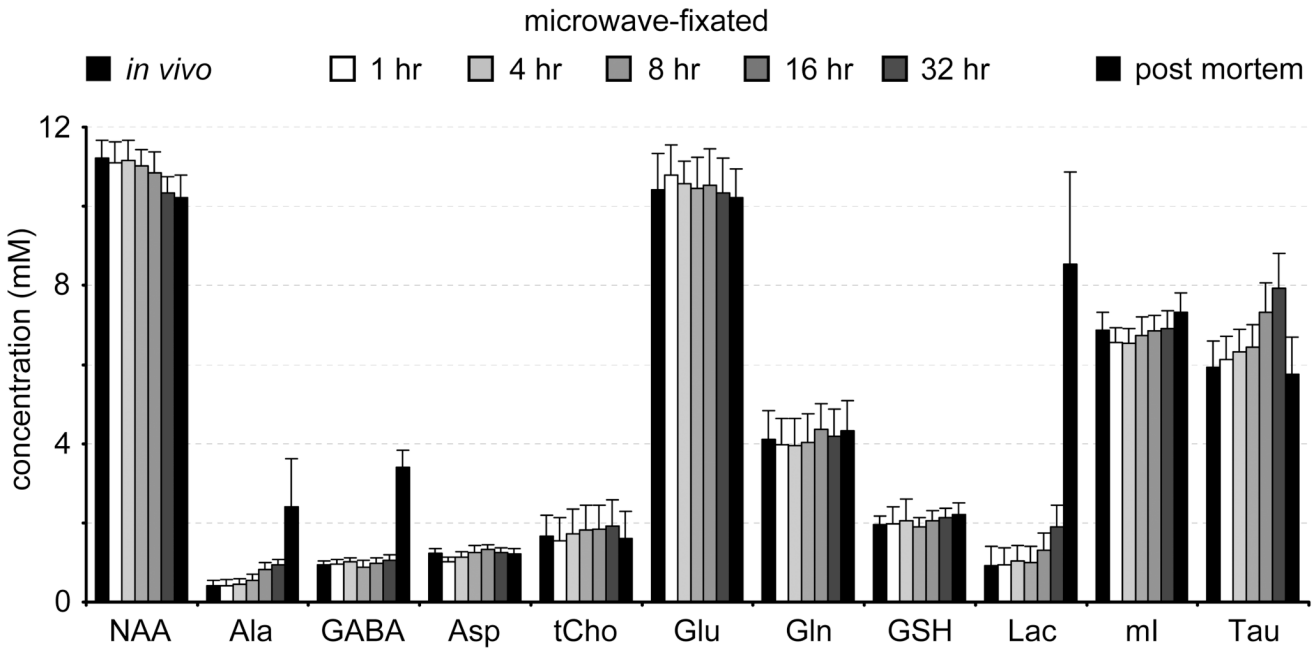

Figure 4.

Absolute metabolite concentrations as obtained from the ^{1}H NMR spectrum acquired on rat brain *in vivo* (black column, left), on rat brain at 1, 4, 8, 16 and 32 hours following microwave-irradiation and on rat brain post mortem (5% halothane, black column, right). For all conditions an internal total creatine concentration of 10 mM was assumed.

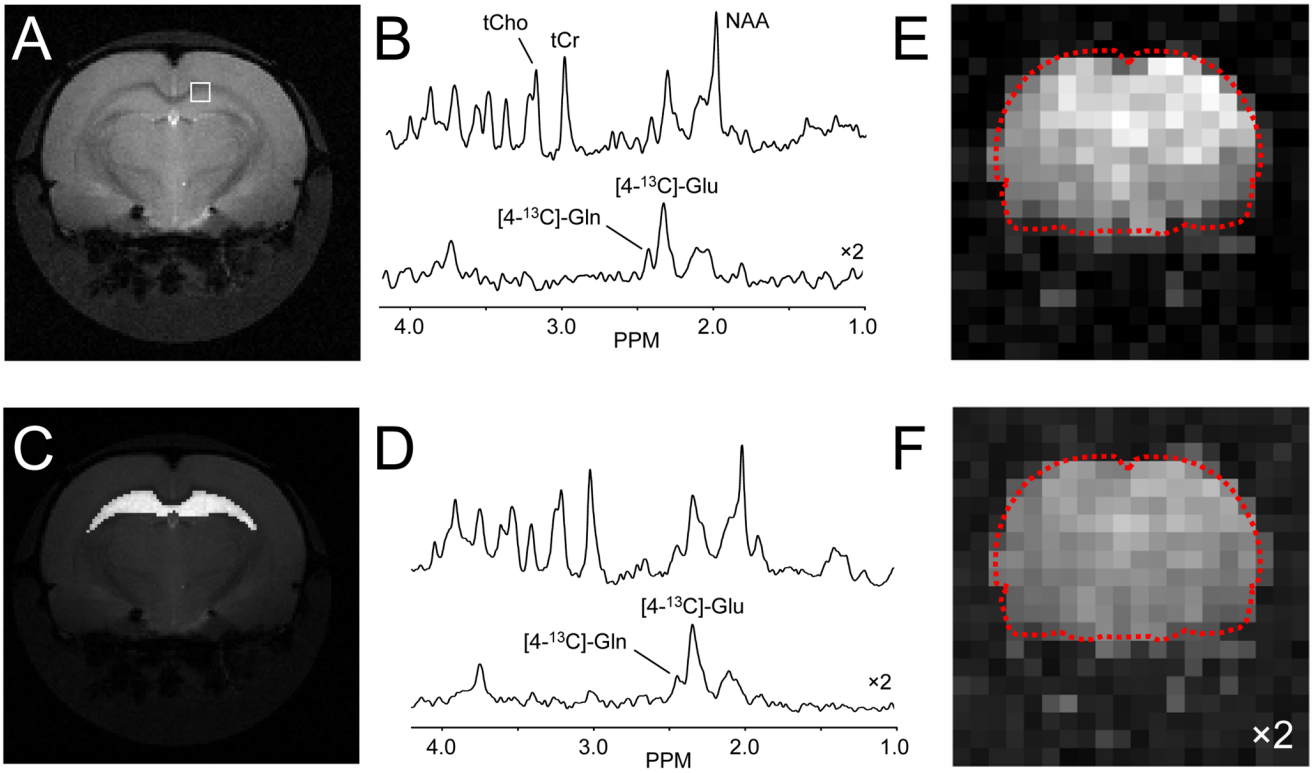

Figure 5.

Multi-slice ^{1}H-[^{13}C]-MRSI on microwave-irradiated rat brain following 2 hours of [1,6-$^{13}C_2$]-glucose infusion. (B) 1 μL volume acquired from the position indicated in (A) showing non-edited (top) and edited ^{1}H-[^{13}C] (bottom) spectra. Regional analysis, e.g. hippocampus as indicated in (C), allows the calculation of high-sensitivity spectra (D) from well-defined regions (see Section C5 for details). (E/F) Spatial map of (E) [4-^{13}C]-glutamate and (F) [4-^{13}C]-glutamine levels (a.u.) obtained by simple (absolute-valued) integration.

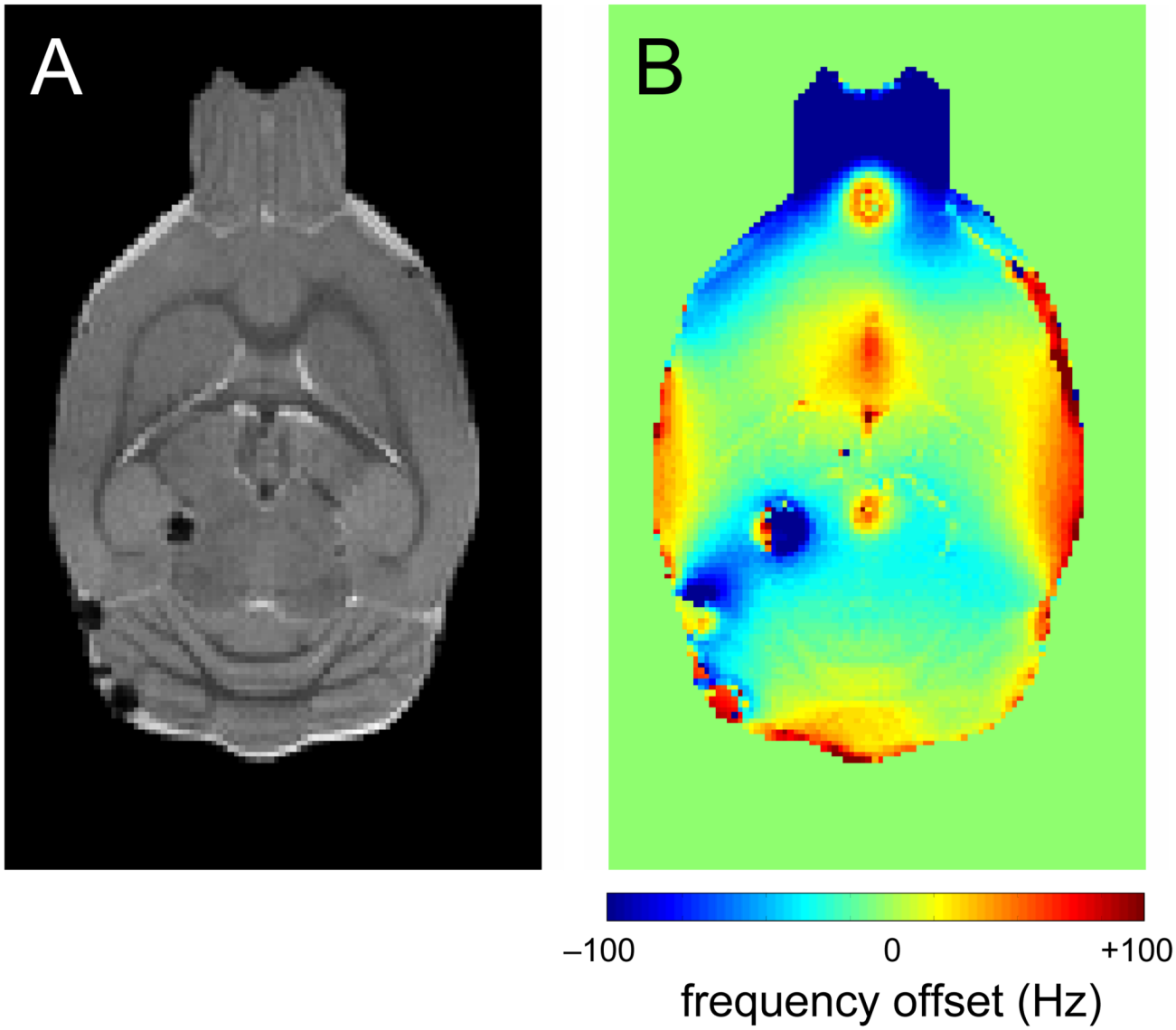

Figure 6.
The effect of microwave-related air bubbles. (A) Coronal spin-echo MR image and (B) B_0 map from microwave-irradiated rat brain. While the spin-echo image is relatively unaffected by small air bubbles formed during FBMI, the magnetic field homogeneity surrounding the bubbles has greatly decreased.